Non-linear vibrational response of Ge and SiC membranes

L. Q. Zhou, G. Colston, M. J. Pearce, R. G. Prince, M. Myronov, D. R. Leadley, O. Trushkevych, and R. S. Edwards[a)]
Department of Physics, University of Warwick, Coventry CV4 7AL, United Kingdom

(Received 30 March 2017; accepted 21 June 2017; published online 6 July 2017)

Characterisation of membranes produced for use as micro-electro-mechanical systems using vibrational techniques can give a measure of their behaviour and suitability for operation in different environments. Two membranes are studied here: germanium (Ge) and cubic silicon carbide (3C-SiC) on a silicon (Si) substrate. When driven at higher displacements, the membranes exhibit self-protecting behaviour. The resonant vibration amplitude is limited to a maximum value of around 10 nm, through dissipation of energy via higher harmonic vibrations. This is observed for both materials, despite their different Young's moduli and defect densities. *Published by AIP Publishing*. [http://dx.doi.org/10.1063/1.4991537]

Membranes show excellent promise for use as micro-electro-mechanical systems (MEMS). By removing the influence of substrate effects, their speed of response and sensitivity can be significantly improved.[1–5] Membranes formed of different materials on a Si substrate, where part of the substrate is removed to form a free-standing membrane, have many potential applications. For example, Ge has high hole mobility and offers excellent electrical properties, but can be fragile as a membrane, leading to problems with sensor longevity.[2–4] An alternative is to use SiC on Si. SiC has hardness close to that of diamond and is much more suitable for use as sensors in hostile environments.[6–10] The process of producing membranes often leads to a residual stress within the membrane due to the mismatch in lattice parameters or thermal expansion coefficients of the component layers.[11]

Membranes have been characterised using contact techniques, such as bulge testing in an atomic force microscope,[12] while in recent years, there has been a move towards non-contact testing, including Raman spectroscopy and curvature measurements.[8] Resonant vibration measurements are also starting to see more applications, and involve vibrating a membrane and using a laser interferometer or vibrometer to study its resonant modes.[1,12–17] Previous measurements and calculations have predominantly measured small amplitude membrane vibrations, where the vibrations can be approximated as being in the linear regime.[1,12,18,19] However, if the vibration amplitude is greater than a critical value, bending and stretching during vibration becomes important.[5,20] This leads to a complex frequency response with higher harmonics. Membranes have been modeled as Duffing oscillators (non-linear resonators),[21,22] but the effect of large amplitude oscillations on their operation as MEMS or resonators has not been considered.

The resonant vibration frequencies of thin films can be governed primarily by elasticity (dominated by bending stiffness) or by tensile stress (dominated by tension applied along its boundary).[18,19,23,24] For the case of tensile stress, the equation of motion is

$$h\rho\ddot{z} = h\sum_{ij}\sigma_{ij}\frac{\partial^2 z}{\partial x_i \partial x_j}, \tag{1}$$

where h is the membrane thickness, ρ is the density, z the out-of-plane deflection, and σ_{ij} the stress tensor of the membrane.[1,15,25] For small deflection amplitudes the stress is constant, given by the static pre-stress, and therefore, the motion is approximately linear. The resonant frequencies of a rectangular membrane in this regime (without considering air damping) are given by

$$f_{mn} = \frac{1}{2}\sqrt{\frac{\sigma}{\rho}\left(\frac{m^2}{l_x^2}+\frac{n^2}{l_y^2}\right)}, \tag{2}$$

where σ is the material biaxial stress, l_x and l_y are the membrane lateral dimensions, and n and m represent the mode number.[18,19] These equations apply where tensile stress dominates, and the resonant frequencies measured show that this is the case for both materials studied here.

Two sets of square membranes were investigated in this study, both using Si as a substrate. The first set of membranes was formed from suspended Ge and the second set from suspended cubic SiC (3C-SiC). 3C-SiC and Ge epilayers were heteroepitaxially grown on 100 mm diameter Si (001) substrates using an industrial type ASM epsilon 2000 reduced pressure chemical vapour deposition system.[2,26] The Ge epilayer was grown to a thickness of 700 ± 12 nm with a threading dislocation density (TDD) of $\sim 10^7\,\mathrm{cm}^{-2}$. The 3C-SiC epilayer was grown to 685 ± 15 nm thickness and was dominated by stacking faults emanating from the interface of the 3C-SiC and Si due to the large lattice mismatch (19.7%). The density of these stacking faults decreases with epilayer thickness due to self-annihilation and the sample exhibited a stacking fault density of $\sim 10^5\,\mathrm{cm}^{-1}$ at its surface as measured using cross sectional TEM.[8] The residual tensile strain of the 3C-SiC epilayer was measured to be $0.11 \pm 0.03\%$ through the acquisition of symmetric and asymmetric X-ray diffraction reciprocal space maps.[7] The thickness (measured using white light reflectometry) has a maximum error consisting of ± 5 nm due to

a)Electronic mail: r.s.edwards@warwick.ac.uk

membrane roughness for 3 C-SiC, and ±2 nm for Ge, and an uncertainty of 10 nm on the thickness due to non-uniformity of the membrane. To fabricate the membranes, the underside of the Si substrate was patterned with photoresist and subjected to anisotropic wet etching in tetramethylammonium hydroxide, as both Ge and SiC show high resistivity to this etching material. The membranes were then cleaned in deionised water and isopropanol.[7,26]

Previous strain measurements have been performed on Ge and 3C-SiC using micro-XRD techniques and showed that while Ge membranes exhibit a slight increase in tensile strain due to tilting at the membrane edges, 3C-SiC membranes undergo slight relaxation due to the reduction in thermally induced strain between the 3C-SiC and Si substrate.[1–3,7] The main samples for which results are presented here are a square Ge membrane of lateral dimensions of 955 μm, and a square 3C-SiC membrane of lateral dimensions 1470 μm.

Vibrations of the membranes were studied over a frequency range of 40–600 kHz. Vibrations were generated using a ring-shaped piezoelectric transducer which was excited using a continuous sinusoidal AC voltage from a function generator, with vibrations coupled through the Si substrate into the membrane using solvent-free glue (Fig. 1), with measurements repeatable after pressure cycling. Deflection of the suspended membrane was measured using a two-wave mixer laser interferometer (Intelligent Optical Systems) with a wavelength of 1550 nm. This measures the out-of-plane displacement and has a bandwidth of 125 MHz. All measurements were done following the membranes reaching thermal equilibrium to reduce heating effects from absorption of the measurement laser, with thermal equilibrium confirmed using a thermal imaging camera. The membranes were placed inside a vacuum chamber, enabling scans to be done at atmospheric pressure and at a reduced pressure of 1.4×10^{-3} mbar, at which the damping effects of the air are significantly reduced.[1] A ring-shaped transducer is chosen, as at atmospheric pressure it minimises any contribution from pressure changes or air movement from directly underneath the membrane, and as no seal is formed between transducer and substrate/membrane the pressure is equalised above and below the membrane.

Three types of measurements were made: (i) scanning in frequency, with the laser interferometer spot at a fixed position on the membrane (at the centre or quarter-diagonal on the membrane in order to be sensitive to most resonant modes[1]); (ii) full two-dimensional scanning to image the resonant modes; and (iii) changing excitation voltage for the piezoelectric transducer and measuring displacement at an antinode.

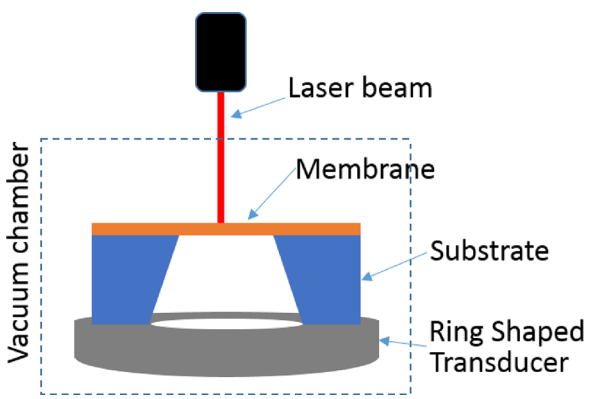

FIG. 1. Measurement set-up (not to scale; membrane is much smaller than shown).

Figure 2 shows a frequency scan for the Ge membrane taken at reduced pressure, along with two-dimensional scans of several modes measured at atmospheric pressure. The 1:1 resonance of this membrane is at 153.09 kHz. The inset mode images were produced by measuring the peak-to-peak displacement at each position during a 2D scan, with the magnitude plotted on a colour scale. The lines around the edges of some of the images correspond to the membrane edges.

The Ge and SiC samples all behave as membranes, despite their very different Young's moduli. Tensile stress can be found by measuring the mode frequencies and comparing them to Eq. (2), allowing for atmospheric damping. For the 955 μm lateral dimensional Ge membrane, the stress is calculated to be 0.228 ± 0.008 GPa, which is in good agreement with previous measurements and calculations based on relaxation and lattice mismatch.[1] For the 3C-SiC membrane, the stress is 0.423 ± 0.007 GPa. From the measurements of strain reported in Ref. 7 and Young's modulus results from Ref. 6, the stress should be in the range of 0.24–0.70 GPa. This measurement provides the average stress, and is in very good agreement. The higher stress in the 3C-SiC membrane compared to the Ge membrane is due to the 3C-SiC having a higher thermal expansion coefficient and larger lattice mismatch with the Si substrate during growth.[7] A summary of results is given in Table I.

The maximum vibration displacement of the membrane depends on the resonant mode shape and the coupling of the vibrations into the membrane; better coupling between transducer and membrane will give higher displacements for a set driving voltage. The displacement of the transducer itself during operation depends approximately linearly on its driving voltage at each frequency. The displacement of the membrane should follow the linear behaviour for low amplitude displacements, with the slope dependent on the coupling

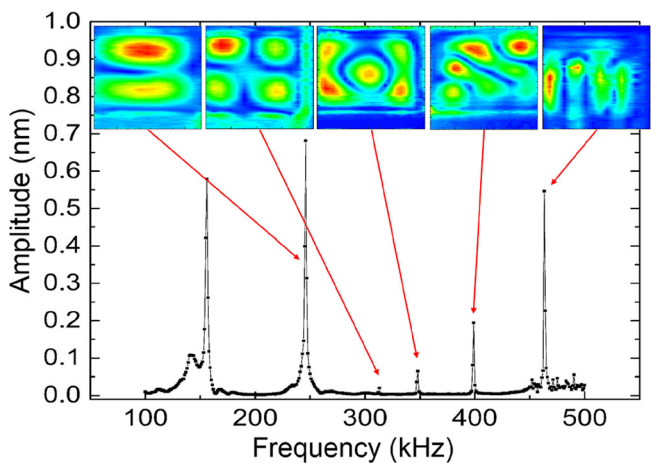

FIG. 2. Frequency scan on the Ge membrane at reduced pressure. The insets show two-dimensional scans measured for the identified modes at atmospheric pressure.

TABLE I. Summary of membrane properties.

	Ge	SiC
Lateral dimensions (μm)	955	1470
Thickness (nm)	700 ± 12	685 ± 15
Residual stress (GPa)	0.228 ± 0.008	0.423 ± 0.007
Young's moduli (GPa)	102.11 (Ref. 30)	300–500 (Ref. 6)
Q-factor (room pressure) (low pressure)	10	25
	408	1349
1:1 freq. (low pressure) (kHz)	153.09	177.19
1:2 freq. (low pressure) (kHz)	242.30	279.75
1:3 freq. (low pressure) (kHz)	341.40	396.01
Critical displacement (nm)	10.4 ± 0.1	10.8 ± 0.1

between transducer and sample. Figures 3(a) and 3(c) show this linear relationship for two samples: (a) Ge membrane, 1:1 mode at 153.09 kHz; (c) 3C-SiC membrane, 1:1 mode at 177.19 kHz; both measured at the centre of the membrane at atmospheric pressure. The 3C-SiC membrane shows larger amplitude vibrations overall, but this is due to better coupling between the transducer and the Si substrate, and the frequency-dependent piezoelectric transducer response.[1] The inset for (c) shows the mode shape at the fundamental frequency.

When measurements are performed at low pressures the effect of atmospheric damping is reduced, the quality (Q-) factors of the resonances increase, and higher amplitude oscillations are possible.[27–29] The Q-factor for the fundamental resonance increases from 10 at atmospheric pressure to 408 at 1.4×10^{-3} mbar for Ge, and from 25 to 1349 for 3C-SiC. Figures 3(b) (Ge membrane) and 3(d) (3C-SiC membrane) show membrane displacements at a pressure of at 1.4×10^{-3} mbar, along with the mode shapes for 3C-SiC at the fundamental frequency. A significant change in behaviour is observed compared to the measurements at atmospheric pressure. The relationship between displacement and voltage is approximately linear until a critical displacement is reached (10.4 ± 0.1 nm in Ge and 10.8 ± 0.1 nm in 3C-SiC), after which the amplitude is reduced. The coupling between the vibration of the transducer and the vibrational mode of the membrane can be very complex. Maximum care was taken to ensure that coupling between the transducer and the membrane remained constant. Due to the use of a ring-shaped transducer and solvent-free glue to form a good bond between transducer and substrate, boundary conditions between the transducer and the membrane are not expected to change as a result of changing pressure. Therefore the observed differences are primarily due to the removal of air damping. Repetition of the measurements on different membranes of both materials show an approximately 20% variation in critical displacement. It is not intuitive that the critical displacements should be so similar for the membranes, as the stress is a factor of 1.86 different. However, the membranes have different lateral dimensions; the gradient of the membrane displacement is 1.54 times larger for the Ge than the 3C-SiC membrane, overcoming the effect of the stress difference.

Figures 4(a)–4(d) show raw vibration data for the 3C-SiC membrane measured at 1.4×10^{-3} mbar for several different transducer driving voltages. At low voltages, and hence small membrane displacements, the vibration pattern is close to the sinusoidal input from the function generator. As the voltage is increased, moving from 16 to 36 mV, the signals increase in amplitude and start to show deviation from sinusoidal. As the voltage increases, shown in part (c) of the figure, the amplitude measured at the antinode position drops as vibration energy moves into the higher harmonic

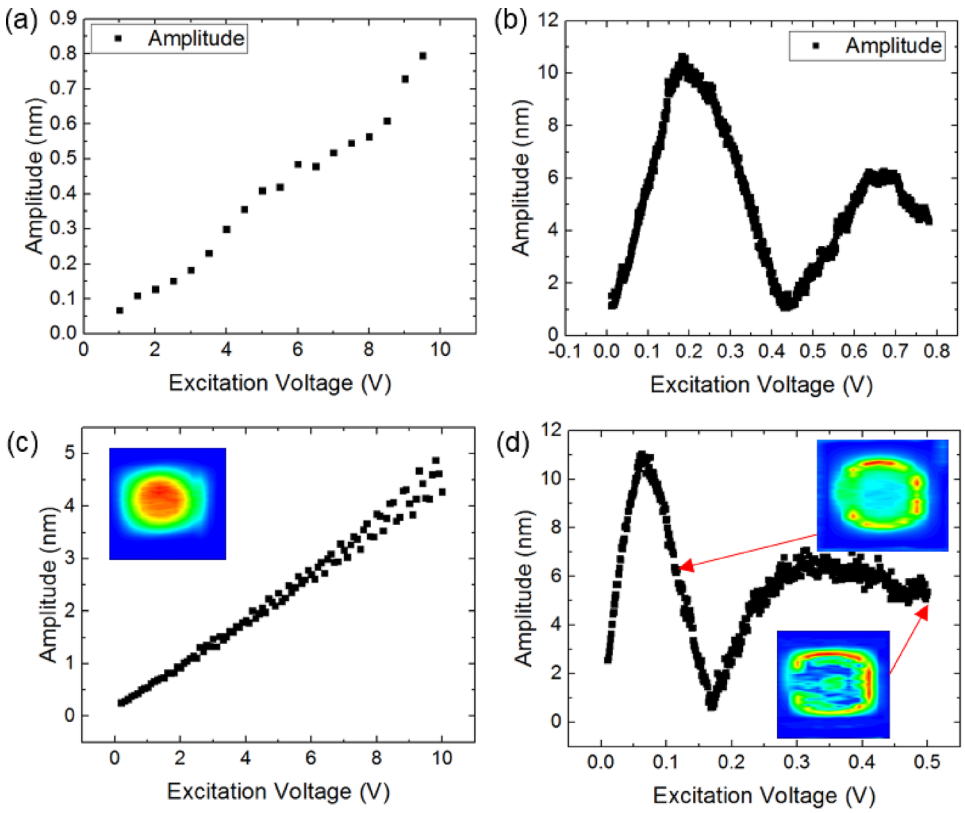

FIG. 3. Measured antinode displacements. Ge membrane, 1:1 mode at 153.09 kHz, at (a) atmospheric pressure and (b) 1.4×10^{-3} mbar. 3C-SiC membrane, 1:1 mode at 177.19 kHz, at (c) atmospheric pressure and (d) 1.4×10^{-3} mbar. Insets show scans on the 3C-SiC membrane at different voltages.

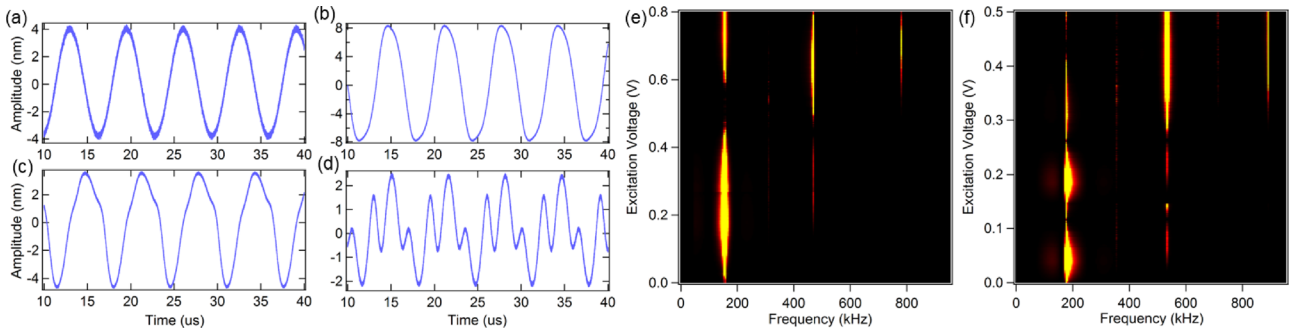

FIG. 4. (a)–(d) 3C-SiC membrane, raw vibration data for the 1:1 mode at voltages of 16, 36, 140, and 190 mV at 1.4×10^{-3} mbar, at a frequency of 177.19 kHz. (e) and (f) FFTs of the vibration data for different excitation voltages, for (c) Ge membrane and (d) 3C-SiC membrane.

frequencies, and this effect becomes much clearer at higher voltages.

Figures 4(e) and 4(f) show fast Fourier transforms (FFTs) of the raw data for the Ge and 3C-SiC membranes, respectively, plotted as a function of excitation voltage. The colour scale shows the magnitude, with the scale varying from black (low) to yellow (high). The odd harmonics appear preferentially over even harmonics, as expected from geometric considerations. As before, the driving voltage at which the onset of non-linear behaviour is observed is predominantly governed by coupling.

The vibration behaviour of the 3C-SiC membrane was mapped experimentally as a function of time for several modes to show the modified vibration. This was done by performing a 2D scan and measuring the vibration at each point, and forming an image at each time by considering the relative amplitude and phase of the vibration at each measurement point. Figure 5(a) shows snapshots of the measurements at several times during one cycle of vibration for the 3:1 resonance mode in the linear regime, with the mode behaviour close to that of a pure 3:1 mode. Figure 5(b) shows the behaviour for a higher transducer voltage and hence higher displacements, showing the higher harmonics.

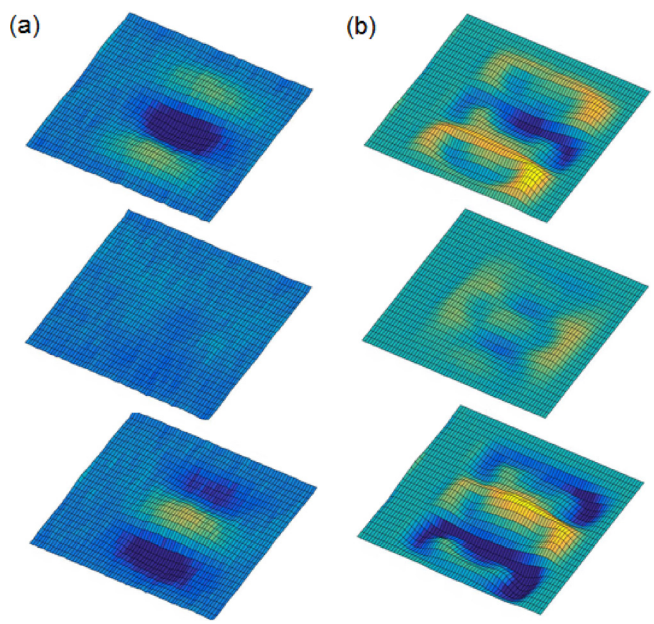

FIG. 5. 3C-SiC membrane; snapshots of the motion of the 3:1 mode at (a) low excitation voltage (linear regime) and (b) high excitation voltage (non-linear), measured at different times during the vibration.

The gradients of the linear sections in Fig. 3 increase by a factor of 779 for the Ge membrane, and 454 for the 3C-SiC membrane. Alongside the different Q-factors, this shows that air damping has a larger effect on the Ge membrane. Coupling to the piezoelectric transducer remains predominantly unchanged for each membrane during pressure cycling and hence does not contribute to the observed differences in the amplitude increase. The behaviour, however, shows that the samples do not behave as perfect membranes—there is some effect due to the elastic properties of the different materials forming the membranes. There is no clear rule on when stress is high enough for the structure to behave like a membrane. With the low residual stresses in these materials, the frequency response is described well by membrane theory.[19] However, other parameters, such as the Q-factors, displacement response, and the early onset of non-linear behaviour are not clearly membrane-like. These parameters appear to be affected by the elastic behaviour of the membranes, which depends on the material properties and intrinsic structure (e.g., defect density).

The Ge and 3C-SiC membranes could offer greater functionality than current membranes used as MEMS, and hence would have more varied uses and applications.[3,26] Some applications entail large vibrations and acceleration (e.g., sensors on space missions), and there is a requirement that such sensors are sufficiently robust. This work shows that these membranes exhibit self-protecting behaviour, limiting their maximum displacement amplitude, by dissipating energy via higher harmonic vibrations. The externally applied strain due to the displacement of the centre of the membrane in the 1:1 resonance mode is extremely small, of the order of 10^{-10} Pa, due to the displacements being much smaller than the lateral dimensions.[31] The consequences of the non-linear vibrational response on the mechanical stability and longevity of such membranes are positive; however, the effect of vibration in both the linear and nonlinear regimes on the electronic properties of the films must be carefully considered. Where these membranes are to be used as MEMS, a measurement of the critical displacement enables identification of constraints that must be placed on their measurement capabilities to ensure that they are always operating in the linear regime, where this is fundamental to their capabilities.

Membrane production was supported by the EPSRC Platform Grant No. EP/J001074/1 and by the University of

Warwick's Higher Education Innovation Fund. Equipment for membrane characterisation was provided through European Research Council Grant No. 202735, and EPSRC Grant No. EP/1031979/1.

[1]O. Trushkevych, V. A. Shah, M. Myronov, J. E. Halpin, S. D. Rhead, M. J. Prest, D. R. Leadley, and R. S. Edwards, Sci. Technol. Adv. Mater. **15**(2), 025004 (2014).
[2]V. A. Shah, M. Myronov, C. Wongwanitwatana, L. Bawden, M. J. Prest, J. S. Richardson-Bullock, S. Rhead, E. H. C. Parker, T. E. Whall, and D. R. Leadley, Sci. Technol. Adv. Mater. **13**, 055002 (2012).
[3]V. A. Shah, S. D. Rhead, J. E. Halpin, O. Trushkevych, E. Chávez-Ángel, A. Shchepetov, V. Kachkanov, N. R. Wilson, M. Myronov, J. S. Reparaz *et al.*, J. Appl. Phys. **115**(14), 144307 (2014).
[4]A. Dobbie, M. Myronov, R. J. H. Morris, A. H. A. Hassan, M. J. Prest, V. A. Shah, E. H. C. Parker, T. E. Whall, and D. R. Leadley, Appl. Phys. Lett. **101**, 172108 (2012).
[5]A. C. Barnes, J. Lee, P. T. Rawlinson, P. X. L. Feng, and C. A. Zorman, in *Proceedings of the IEEE Sensors* (2012), pp. 12–15.
[6]H. P. Phan, D. V. Dao, K. Nakamura, S. Dimitrijev, and N. T. Nguyen, J. Microelectromech. Syst. **24**, 1663 (2015).
[7]G. Colston, S. D. Rhead, V. A. Shah, O. J. Newell, I. P. Dolbnya, D. R. Leadley, and M. Myronov, Mater. Des. **103**, 244–248 (2016).
[8]F. Iacopi, G. Walker, L. Wang, L. Malesys, S. Ma, B. V. Cunning, and A. Iacopi, Appl. Phys. Lett. **102**, 011908 (2013).
[9]G. Ferro, CRC Crit. Rev. Solid State Sci. **40**, 56 (2015).
[10]M. Mehregany and C. A. Zorman, Thin Solid Films **355–356**, 518 (1999).
[11]Y. Sakashita and H. Segawa, J. Appl. Phys. **73**, 7857–7863 (1993).
[12]X. Zhang, C. Neumann, P. Angelova, A. Beyer, and A. Golzhauser, Langmuir **30**, 8221–8227 (2014).
[13]C. H. M. Jenkins and U. A. Korde, J. Sound Vib. **295**, 602–613 (2006).
[14]S. Ma, S. Wang, F. Iacopi, and H. Huang, Appl. Phys. Lett. **103**(3), 031603 (2013).
[15]R. Waitz, S. Nößner, M. Hertkorn, O. Schecker, and E. Scheer, Phys. Rev. B **85**(3), 035324 (2012).
[16]X. Zhang, R. Waitz, F. Yang, C. Lutz, P. Angelova, A. Golzhauser, and E. Scheer, Appl. Phys. Lett. **106**, 063107 (2015).
[17]S. Hyun, W. L. Brown, and R. P. Vinci, Appl. Phys. Lett. **83**, 4411 (2003).
[18]L. E. Kinsler, A. R. Frey, A. B. Coppens, and J. V. Sanders, *Fundamentals of Acoustics* (Wiley, 1999), Vol. 1.
[19]A. W. Leissa, *Vibration of Plates* (National Aeronautics and Space Administration, 1969).
[20]N. Yamaki and M. Chiba, Thin-Walled Struct. **1**, 3–29 (1983).
[21]S. Zaitsev, O. Shtempluck, E. Buks, and O. Gottlieb, Nonlinear Dyn. **67**, 859–883 (2012).
[22]Y. Yang, E. J. Ng, P. M. Polunin, Y. Chen, I. B. Flader, S. W. Shaw, M. I. Dykman, and T. W. Kenny, J. Microelectromech. Syst. **25**, 859–869 (2016).
[23]A. Fartash, I. K. Schuller, and M. Grimsditch, J. Appl. Phys. **71**(9), 4244 (1992).
[24]K. F. Graff, *Wave Motion in Elastic Solids* (Dover, Mineola, NY, 1975).
[25]R. Waitz, C. Lutz, S. Nössner, M. Hertkorn, and E. Scheer, Phys. Rev. Appl. **3**, 044002 (2015).
[26]M. Myronov, G. Colston, and S. Rhead, G.B. patent application GB1513014.9 (23 July 2015).
[27]L. Khine and M. Palaniapan, J. Micromech. Microeng. **19**(1), 015017 (2009).
[28]G. Q. Wu, D. H. Xu, B. Xiong, and Y. L. Wang, Microelectron. Eng. **103**, 86 (2013).
[29]B. Kim *et al.*, J. Microelectromech. Syst. **17**(3), 755 (2008).
[30]S. L. Rumyantsev, M. E. Levinshtein, and M. S. Shur, *Properties of Advanced Semiconductor Materials* (Wiley, 2001).
[31]S. Rohmfeld, M. Hundhausen, L. Ley, C. A. Zorman, and M. Mehregany, J. Appl. Phys. **91**, 1113 (2002).